Mineralogy of the Manipur Ophiolite Belt, North East India: implications for mid-oceanic ridge and supra-subduction zone origin

Thungyani N. Ovung[1,]*, Jyotisankar Ray[1], Xueming Teng[2], Biswajit Ghosh[1], Madhuparna Paul[1], Proloy Ganguly[1], Saradee Sengupta[1] and Supriyo Das[1]

[1]Department of Geology, Calcutta University, 35 B.C. Road, Kolkata 700 019, India
[2]School of Earth Sciences and Resources, China University of Geosciences Beijing, 29 Xueyuan Road, Beijing 100083, China

Mineralogical studies on the mantle and crustal sections of the Manipur Ophiolite Belt (MOB) lead to important findings pertaining to its genesis and controlling tectonic milieu. The wide compositional gap in the Cr# and Mg# content of spinel in the mantle peridotites of MOB implies upper mantle melting in two different tectonic settings. The tectonic discrimination diagrams based on spinel chemistry indicate a mid-oceanic ridge (MOR) origin for the high-Al spinel peridotites and a supra-subduction zone origin for the high-Cr spinel peridotites. The pyroxenite mantle dyke, ultramafic cumulate and pillow-basalt record temperature in the range of 600–1030°C, 600–800°C and 700–1005°C respectively. Plotting of clinopyroxene composition of pillow-basalt in the TiO_2–Na_2O–SiO_2/100 (wt%) tectonic discrimination diagram, implies a subduction-related origin of the basalts. Experimental studies on the serpentine stability indicate that it was dominantly affected by high temperature-low deformation setting.

Keywords: Mineralogical study, ophiolite belt, pyroxenite mantle dyke, pyroxene thermometry.

THE Manipur Ophiolite Belt (MOB) which is a part of the Naga-Manipur Ophiolite Belt (NMOB) has been studied by several workers[1–12]. It occurs within the NNE–SSW trending Indo-Myanmar Orogenic Belt (IMOB), a remnant of the Tethyan Ophiolite in the Alpine-Himalayan orogenic system[13–16]. Initially, it was proposed that several subduction processes were involved in the generation of this ophiolite belt resulting from the convergence of the Indian plate with the Myanmar plate[14,17–21]. However, the tectonic processes involved in this are still controversial. Recent studies have suggested that the peridotites of MOB are the residues remaining after low-degree partial melting of spinel–peridotite mantle at mid-oceanic ridge environment[3,5–7]. The mafic volcanics are also suggested to be derived from a heterogeneous mantle source at a spreading ridge zone[12].

Implications on the origin of these rocks can be made through the study of the constituent primary mineral phases. Therefore, in this study, we present field observations of MOB and its mineralogical aspects to provide a brief overview on its petrogenesis. Experimental study was also done on the serpentine grains to understand the serpentine stability in terms of regional tectonic frame.

In the Indo-Myanmar Ranges, the ophiolitic rocks occur in two parallel belts (Eastern belt and Western belt) along the eastern margin of the Indian plate. The Eastern belt passes through central Myanmar, Sumatra and Java, whereas the Western belt passes through Nagaland, Manipur, western Myanmar and Andaman islands[1] (Figure 1, inset).

MOB which is the southern extension of Naga Hills Ophiolite (NHO) shows an easterly dipping thrust contact with the underlying Disang and Barail flysch sediments (Upper Cretaceous–Upper Eocene), whereas the eastern part is overthrusted by continental metamorphic rocks known as the Naga metamorphics[22]. NHO and its associated rocks are broadly classified into three distinct tectono-stratigraphic units from east to west, viz. (1) the Nimi Formation, (2) NHO and (3) the Disang Formation. A fourth tectono-stratigraphic unit known as the Jopi Formation is a post-orogenic molasse that consists of ophiolite-derived sediments, and occurring as a cover sequence over NHO[9].

The study area is confined within Jessami in the north and Moreh in the extreme south (Figure 1). It consists of mantle peridotite (serpentinite), pyroxenite mantle dyke, ultramafic cumulate and mafic intrusives and pillow basalt which are overlain by pelagic sediments. The ophiolitic rocks are absent in the Jessami–Marem and Shangshak–Phungyar sectors.

Mantle peridotite is the dominant lithotype which occupies the basal unit. They are mostly highly weathered and serpentinized. Few fresh samples of harzburgite, lherzolite, wehrlite and dunite are found in Sirohi, Phangrei, Gamnom, Maku, Kamjong, Lungpha and Khudenthabi. Intrusive dyke solely restricted within the mantle-borne restites has been referred to in the literature as 'deep dykes' or mantle dykes[23]. Pyroxenite mantle dyke intruding the mantle peridotite is found at Gamnom in the present study area. It displays a sharp contact with the mantle peridotite, cutting across its foliation planes. The deformed mantle peridotites are overlain by the cumulate unit. The lower cumulate sequence is represented by ultramafic cumulates like harzburgite and lherzolite, and the upper cumulate sequence is represented by gabbro. Ultramafic cumulate rocks are predominantly observed in the Gamnom–Kamjong and Moreh–Khudenthabi sectors. Mafic intrusives like the layered gabbro are scantily distributed in and around Gamnom. They exhibit banding of mafic and felsic minerals. The volcanic rocks

*For correspondence. (e-mail: ayani_ovung@yahoo.com)

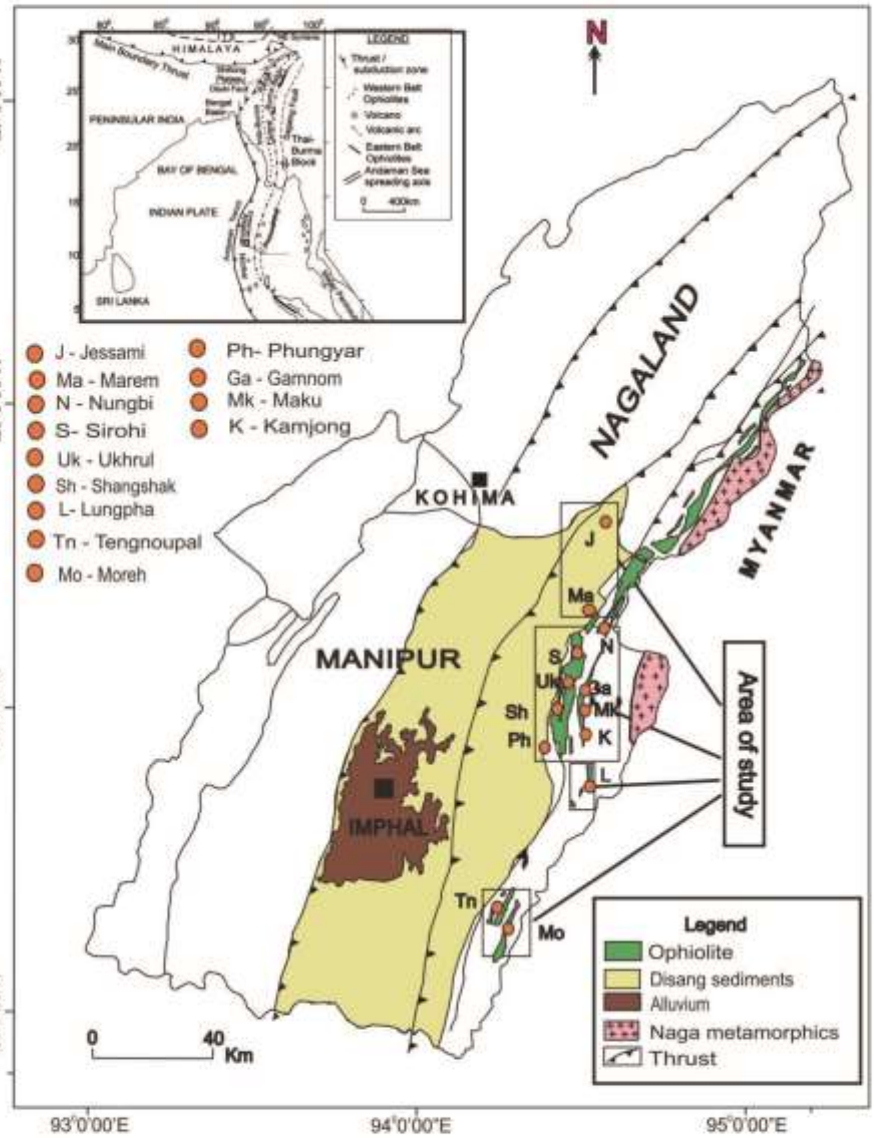

Figure 1. Regional map of the Nagaland–Manipur Ophiolite Belt, North East India (modified from GSI, M.N.C. DRG. No. 42/87). Inset figure by previous worker[1].

show pillow structures with outer chilled margins due to their extrusion under water. They are vesiculated and mostly ferruginized; occasionally traversed by carbonate veins. Radiolarian chert occupies the topmost layer of this ophiolite which is observed in Ukhrul–Nungbi and Gamnom–Shangshak sectors (Figure S1*a–f*, see Supplementary Material online).

For electron probe micro analyses (EPMA), seven well-polished thin sections corresponding to different lithounits of MOB were analysed using the Cameca SX-100 microprobe at the Geological Survey of India, Kolkata. Accelerating voltage and beam current were 15 kV and 12 nA respectively, with a beam size of 1 μm. Signals used were Na$K\alpha$, Mg$K\alpha$, Al$K\alpha$, Si$K\alpha$, P$K\alpha$, K$K\alpha$, Ca$K\alpha$, Ti$K\alpha$, Cr$K\alpha$, Mn$K\alpha$, Fe$K\alpha$ and Ni$K\alpha$. To minimize the migration and volatilization of the mobile elements (Na, K), the counting time was 2 sec for Na and K, and 5 sec for the other elements (Si, Ti, Al, Fe, Mg and Ca). Natural standards like 'albi' (for determination of SiO_2 and Na_2O), 'apatite' (for CaO and P_2O_5), 'olivine' (for MgO), 'ortho' (for K_2O), 'Al_2O_3', 'Cr_2O_3' and 'Fe_2O_3' were used. For 'Mn', 'Ni' and 'Ti' synthetic standards were applied.

Experimental studies were carried out using silicon carbide furnace and Kanthal wound heating furnace. These were undertaken to understand the stability fields of different varieties of serpentine (corresponding to different temperature domains), in order to constrain their genesis in specific tectonic milieu. In this furnace, we carried out experimental runs at a temperature span of 400–600°C. The temperatures were measured precisely using a Pt_{100}–$Pt_{87}Rh_{13}$ thermocouple and a pyrometer (for further details, see Appendix in Supplementary Material online).

In the mantle peridotites, serpentinization is pervasive. Most of the primary mineral phases have been altered. It consists of relict olivine, orthopyroxene, clinopyroxene, serpentine and accessory minerals like Cr-spinel and magnetite. Nodular chromitite pods are also observed in some harzburgites. Few relict olivine grains are crushed, flattened and often show parallel arrangement. Orthopyroxene occurs as subhedral prismatic grain or as irregular grain with inclusion of fine exsolution lamellae of clinopyroxene. Embayed orthopyroxene phenocrysts are rimmed by fine-grained serpentine. Kink-banding is also observed. Thin magnetite streaks and striations are disposed along some of the clinopyroxene cleavages.

Serpentine grains are mostly lizardite and chrysotile. Lizardite shows mesh-like pseudomorphic texture after olivine, while chrysotile occurs as cross-fibre veinlets transversing the lizardite. Antigorite is present in lesser amount. It occurs as interpenetrative plates and veins, or as scaly aggregates. Cr-spinel occurs as both subhedral to euhedral crystal or as irregular grain with reddish to dark brown colour (Figure S2 a–*f*, see Supplementary Material online). Back-scattered electron (BSE) image shows nodular olivine grains and a large subhedral chrome-spinel (Figure 2 *a*). Modal analyses show that the few less-serpentized tectonites are mostly harzburgite and wehrlite. A few lherzolite and dunite are also observed.

The pyroxenite dyke is a coarse-grained, dark-coloured rock intruding the mantle peridotite. It consists of orthopyroxene, clinopyroxene, serpentine, some relict olivine and accessory opaque minerals. Large subhedral prismatic orthopyroxene grains are dominant. Exsolution clinopyroxene lamellae within the orthopyroxene are common. Figure 2 *b* shows the BSE image of a representative subhedral clinopyroxene grain. Pyroxene and magnetite intergrowth forms symplectite texture.

In the coarse-grained ultramafic cumulate, the primary minerals like orthopyroxene, clinopyroxene and olivine are aligned parallel exhibiting igneous layering. Orthopyroxene occurs as subhedral grains with straight extinction; occasionally showing bastite texture. Minor amount of subhedral–anhedral clinopyroxene is also found. The mafic cumulate (gabbro) consists of plagioclase, clinopyroxene and opaque minerals. Uralitization has converted clinopyroxene to pale green tremolitic amphibole. Optically, these secondary tremolites are readily identifiable with their pale green to dark green pleochroism (Figure S2 *g*, see Supplementary Material online). Zoning in plagioclase is also observed.

The basalt consists of plagioclase, pyroxene and glass. Intersertal and intergranular texture is common where the spaces within the network formed by plagioclase laths are filled with glass and pyroxene grains respectively. At places, large plagioclase phenocrysts cluster to form a glomeroporphyritic texture. The fine-grained microlites exhibit a hyalopilitic texture in the groundmass (Figure S2 *h*, see Supplementary Material online). BSE image shows zoning in K-feldspar grain (Figure 2 *c*).

The topmost part of this ophiolite suite is the radiolarian chert. It shows microcrystalline groundmass represented mainly by microcrystalline chert, few mica grains and

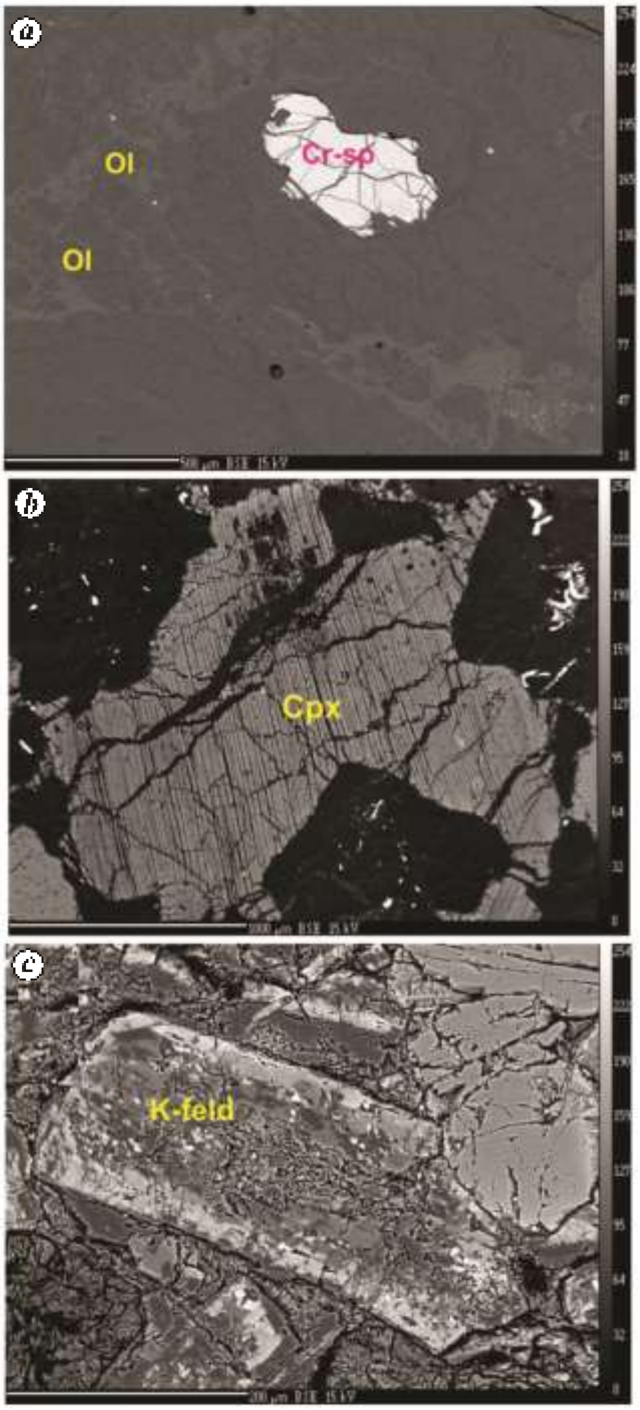

Figure 2. BSE image showing (***a***) a large clinopyroxene grain in the mantle dyke; (***b***) K-feldspar zoning in pillow basalt and (***c***) nodular olivine grains and Cr-spinel in the mantle dyke. Cpx, Clinopyroxene; K-Feld, Potash feldspar and Ol, olivine.

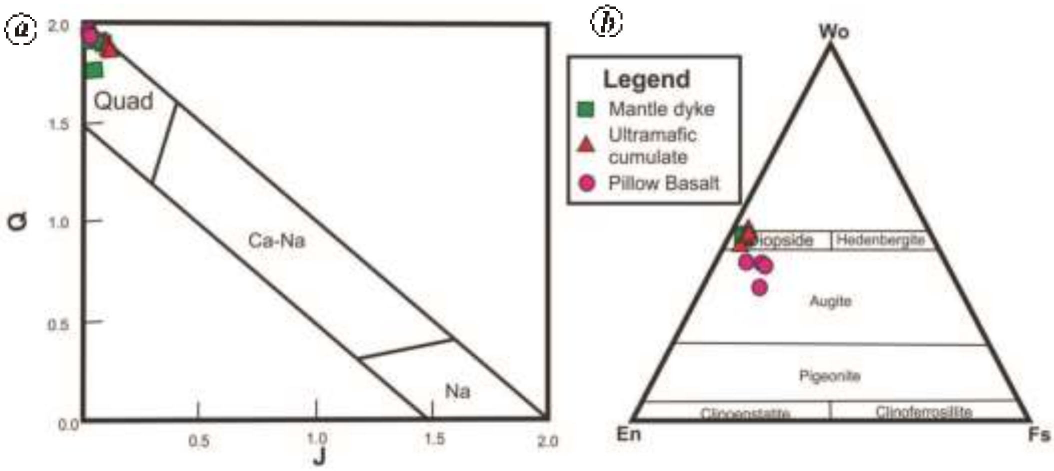

Figure 3. ***a***, Plot of pyroxene data in terms of *Q–J* classification[24]; ***b***, Pyroxene plots in Wo–En–Fs diagram[25].

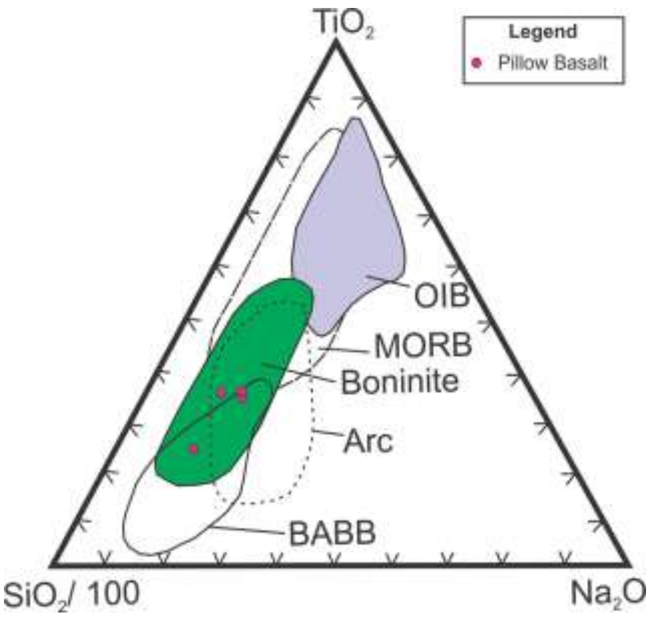

Figure 4. TiO_2–Na_2O–SiO_2/100 (wt%) for discrimination of clinopyroxene from basalt of different tectonic settings[26]. MORB, Mid-ocean ridge basalt; OIB, Ocean-island basalt and BABB, Back-arc basin basalt.

some opaque minerals. Polygonal mosaic structures made of spikes and bars of radiolaria are observed. Secondary carbonate veins traverse the rock.

Representative electron micro probe data of constituent phases namely pyroxene, feldspar, olivine, spinel and serpentine are provided in the Tables S1–S5 (see Supplementary Material online).

Clinopyroxene is characterized by high CaO (14.85–23.78 wt%), SiO_2 (45.4–51.75 wt%) and MgO (15.56–18.29 wt%). The investigated pyroxene data in the *Q–J* classification diagram (Figure 3 *a*), fall within the 'Quad' field[24]. Pyroxene plotting in Wo–En–Fs ternary diagram[25] indicates that they are dominantly diopsidic; a few analyses yielded augitic variety (Figure 3 *b*). Plotting of clinopyroxene of the pillow basalt in the TiO_2–Na_2O–SiO_2/100 (wt%) discrimination diagram[26] implies a subduction-related origin of the basalts (Figure 4).

Feldspar in the pillow basalt is of two types: (a) plagioclase which occurs as a major mineral and (b) K-feldspar which occurs as tiny accessories. In the Or–Ab–An diagram, the compositions of plagioclase are restricted within albite field, whereas the accessory K-feldspar corresponds to sanidine (sanidine has been identified by its lower optic axial angle and absence of micro-perthitic texture). Zoning in the K-feldspar grain (Figure 2 *c*) gives analytical data showing potassium content increasing from the core to the margin.

The investigated olivine has a relatively uniform composition. It shows a narrow range of SiO_2 (38.33–41.68 wt%) and MgO (31.77–38.66 wt%). Fo and Fa range from 82.79 to 95.505 and 4.57 to 17.21 respectively, and therefore correspond to magnesian forsterite and chrysolite variety. The Mg# and Cr_2O_3 values range from 0.828 to 0.955 and 0.19 to 0.95, which is relative to the pyroxene composition.

The spinel group includes both high-Cr and high-Al spinels. The latter are characterized by high Al_2O_3 (42.3–51.66 wt%) and MgO (17.85–19.04 wt%) with relatively low Cr_2O_3 (16.65–25.25 wt%). Cr# [Cr/(Cr + Al)] and Mg# [Mg/(Mg + Fe^{2+})] range from 0.179 to 0.283 and 0.711 to 0.738 respectively. On the other hand, the high-Cr spinels are characterized by high Cr_2O_3 (40.3–57.87 wt%) with low Al_2O_3 (6.71–26.06 wt%) and MgO (6.88–13.61 wt%). Cr# and Mg# range from (0.526 to 0.85) and (0.31 to 0.567) respectively. TiO_2 content of both these spinels is very low (0.03–0.19 wt%). The binary plot of Cr# versus TiO_2 (Figure 5 *a*) indicates that serpentinized peridotites are the likely products of both depleted mantle as well as boninitic magma. The high Cr# (>0.60) and low TiO_2 contents of the high-Cr spinels are most consistent with modern, highly refractory

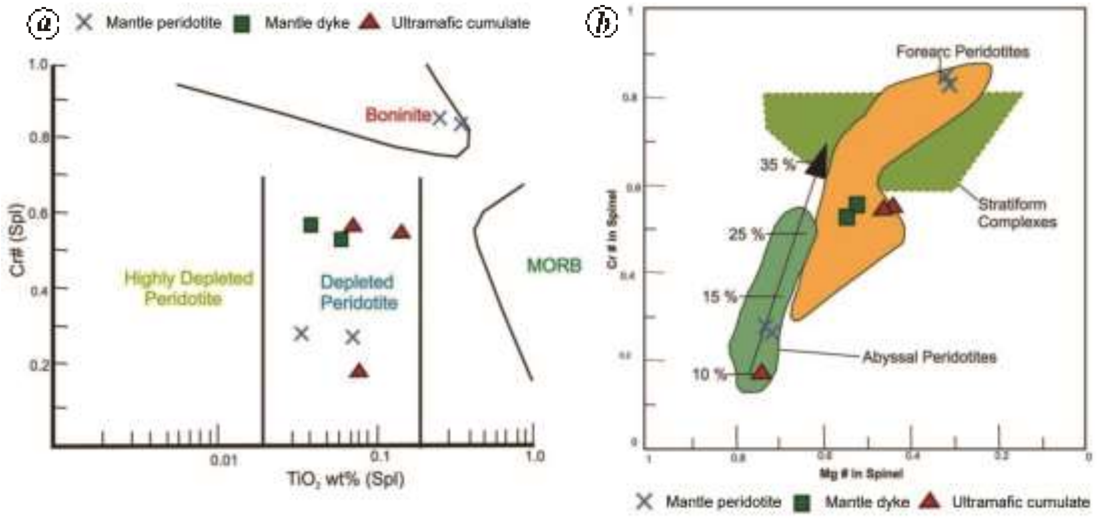

Figure 5. Tectonic discrimination diagrams for spinel: (***a***) Cr# versus TiO_2 diagram for fresh chromian spinels[37–40] and (***b***) Cr# versus Mg# (Mg# = Mg/(Mg + Fe_2)). Fields of abyssal peridotite and stratiform complexes and forearc peridotite are also shown[37,41]. Arrow represents the percentage of partial melting of the host peridotite[41].

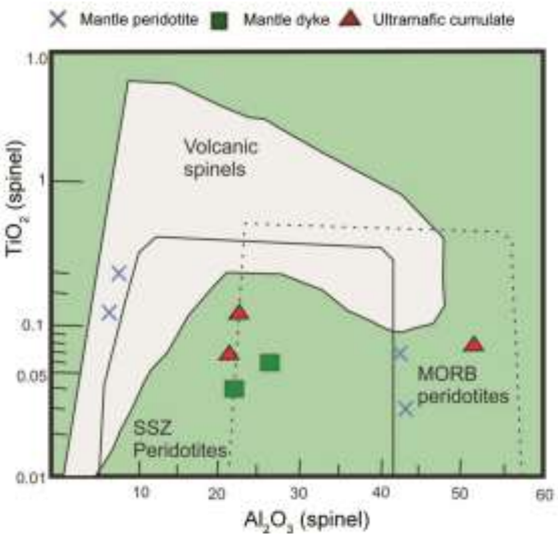

Figure 6. TiO_2 versus Al_2O_3 diagram[42].

forearc peridotites and suggest these rocks had probably developed in a supra-subduction zone (SSZ) environment. Cr# versus Mg# diagram also denotes ‘forearc’ peridotite parentage for the high-Cr spinels. The high-Al spinels are most likely to be produced from the ‘abyssal’ peridotite that underwent ~10–13% partial mantle melting (Figure 5 *b*). The TiO_2 versus Al_2O_3 diagram also implies both mid-oceanic ridge (MOR) and SSZ origin of the peridotites (Figure 6).

Serpentine is characterized by high SiO_2 (33.39–44.01 wt%), MgO (32.13–40.06 wt%) and FeO (2.86–15.38 wt%). In some cases, the Si content of serpentine shows values slightly higher (>2 apfu) than commonly reported, which could be explained by the occurrence of antigorite[27].

An effective method of determining the equilibration temperature can be attained by projecting several end-member components of the calcic-pyroxenes in the pyroxene thermometry diagram[28]. The end-members – Ac (acmite), Jd (jadeite), FeCaTs (iron cations), CrCaTs (chromium cations) and AlCaTs (aluminium cations) need to be recalculated first. When plotted on experimentally determined pyroxene thermal contours, temperatures ranging from 600°C to 1030°C, 600°C to 800°C and 700°C to 1005°C are obtained for the pyroxenite mantle dyke, ultramafic cumulate and basalt respectively (Figure 7).

Clinopyroxene is a common phenocrystal phase in basalts. An effective clinopyroxene geobarometer for basaltic lavas was proposed on the basis of the mineral chemical composition in order to determine the pressure of crystallization of clinopyroxene phenocrysts[29]. Based on this method, the mantle dyke and ultramafic cumulate show equilibration pressure in the range ~2.0–5.5 kbar, while the pillow basalt corresponds to ~1 bar.

Experimental studies at 1atm were carried out on two fresh representative mantle peridotite samples (301A and 312A). Different heating experiments on the selected samples were carried out to understand the stability of the serpentine species. Table 1 provides a summary of the experimental observations. The table explicitly shows transition of different serpentine species in response to increasing temperatures (Figure S3, see Supplementary Material online). This transition enables us to constrain the prevalent deformational milieu.

Spinels from MOR and back-arc basin peridotites generally contain Cr# <0.5, whereas those from forearc peridotites and boninites generally have higher Cr# (up to 0.8 and 0.7–0.9 respectively)[30,31]. Low Cr# (spinel) indicates a moderately fertile character like the Al-rich fertile lherzolite which is the result of small degree of partial

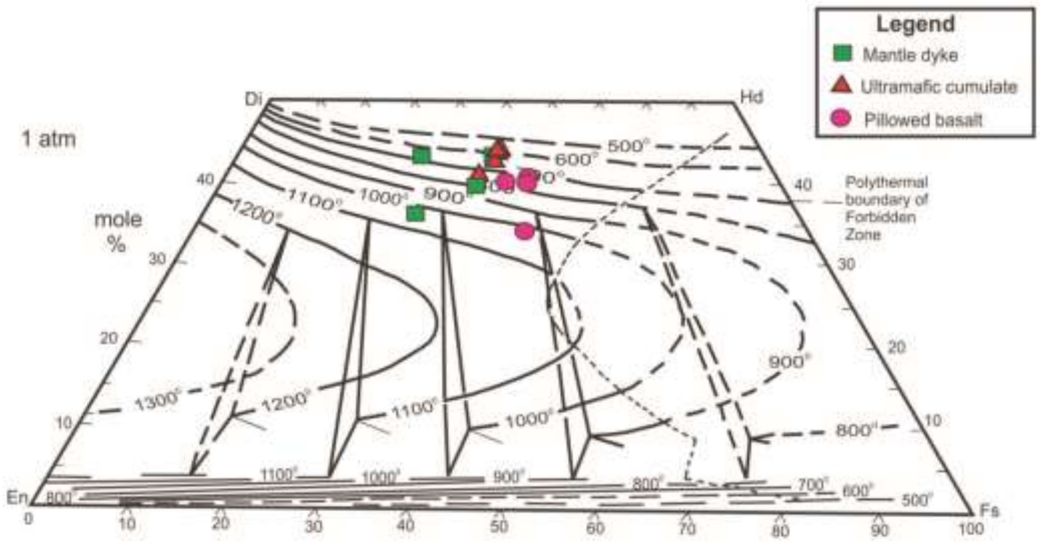

Figure 7. Projection of recalculated pyroxene end member composition in pyroxene thermometry diagram[28] based on data presented in the Table S1 (see Supplementary Material online).

Table 1. Summary of the experimental findings

Temperature (°C)	Temperature run (min)	Observations
Sample no. 301A		
400	30	Serpentine (greenish antigorite) persists.
450	20	Antigorite continues with appearance of light brown variety of serpentine (chrysotile)
500	20	Greenish variety diminishes and yellowish-brown chrysotile variety predominates with rise in temperature.
550	20	Brown chrysotile variety of serpentine predominates; only a few grains of the green variety (antigorite) remain.
600	20	Only brown chrysotile variety of serpentine occurs. Green variety of serpentine (antigorite) is absent (Figure S3 *a*, see Supplementary Material online).
Sample no. 312A		
400	30	Serpentine (greenish antigorite) remains, but its colour changes from green (antigorite) to yellowish brown (chrysotile).
450	20	Yellowish-brown chrysotile continues as in case of the 400°C run.
500	20	Yellowish-brown chrysotile predominates.
550	20	Only coarse, brown chrysotile exists.
600	20	Only brown chrysotile exists (Figure S3 *b*, see Supplementary Material online).

melting, while the high Cr# (spinel) indicates higher degree of partial melting from a subduction zone[32,33]. There is a wide compositional gap in the Cr# and Mg# content of spinel in the mantle peridotites of MOB, which is an implication of upper mantle melting in two different tectonic settings. The tectonic discrimination diagrams based on spinel chemistry indicate an MOR origin for the high-Al spinel peridotites (Cr# = 0.179–0.283 and Mg# = 0.711–0.738) with approximately 10–13% partial mantle melting, and SSZ origin for the high-Cr spinel peridotites (Cr# = 0.526–0.85 and Mg# = 0.310–0.567).

It has been inferred that the pyroxenite dykes in the upper mantle have not been directly crystallized from primary magmas generated by the melting of ultra-depleted mantle; rather, the relevant magmas acquired the signatures of such mantle by reacting and reaching equilibrium with large volumes of variously depleted peridotites during their migration through the mantle[34]. The pyroxene thermometry for the disequilibrium assemblages yielded temperature in the 600–1030°C range for the pyroxenite dyke of MOB. The ultramafic cumulate recorded a comparable 600–800°C thermometric value (however, it segregates at relatively higher temperature).

Clinopyroxene geobarometry gave pressure in the range of ~2.0–5.5 kbar for the pyroxenite dyke and ultramafic cumulate, while the pillow-basalt corresponded to ~1 bar. Pillow basalts equilibrated at a temperature of 700–1005°C, implying their shallow depth formation in the back-arc basin. Clinopyroxene composition from this pillow basalt in the TiO_2–Na_2O–SiO_2/100 (wt%) discrimination diagram[26], also confirms the subduction-related origin of the basalts.

Serpentine stability is also related to mantle depth and subduction-related magmatism[35]. The stability of antigorite may commence below 300°C with dominant mesh structure between 320°C and 390°C (ref. 37). Antigorite-bearing serpentinite may prevail at moderate temperatures, with high deformation setting characterized by intense tectonic activity and major shear stress. The chrysotile on the other hand, represents relatively less deformation and relatively higher temperature zone. It replaced antigorite *in situ* in shear planes most likely at a transitional stage of deformation exhibiting both ductile and brittle fabric in the areas. Experimental studies (Table 1 and Figure S3, see Supplementary Material online) showed transition from antigorite to chrysotile species with increasing temperature. The presence of mostly chrysotile species in the mantle peridotites of MOB indicates that it is dominantly affected by high temperature–lower deformation setting. The present study therefore infers MOR spreading as well as subduction processes for the generation of MOB; almost similar to the situation recorded from Pindos ophiolite[36].

1. Acharyya, S. K., Collisional emplacement history of the Naga-Andaman ophiolites and the position of the eastern Indian suture. *J. Asian Earth Sci*., 2007, **29**, 229–242.
2. Joshi, A. and Vidyadharan, K. T., Lithostratigraphy of the Naga-Manipur Hills (Indo-Burma Range) ophiolite Belt from Ukhrul district, Manipur, India. *Himalayan J. Sci.*, 2008, **5**(7), 73–74.
3. Singh, A. K., High-Al chromian spinel in ultramafic rocks of Manipur Ophiolite Complex, Indo-Myanmar Orogenic Belt: implication for petrogenesis and geotectonic setting. *Curr. Sci*., 2009, **96**(7), 973–978.
4. Devi, L. D. and Singh, I., Geochemical study of peridotites from the Manipur Ophiolite Complex, Northeast India with special reference to their PGE concentration. *J. Geol. Soc. India*, 2011, **77**, 273–279.
5. Ningthoujam, P. S., Dubey, C. S., Guillot, S., Fagio, A. S. and Shukla, D. P., Origin and serpentinization of ultramafic rocks of Manipur Ophiolite Complex in the Indo-Myanmar subduction zone, Northeast India. *J. Asian Earth Sci*., 2012, **50**, 128–140.
6. Singh, A. K., Singh, I., Devi, L. D. and Singh, R. K. B., Geochemistry of Mid-Ocean ridge Mafic intrusive from the Manipur Ophiolitic Complex, Indo-Myanmar Orogenic Belt, NE India. *J. Geol. Soc. India*, 2012, **80**, 231–240.
7. Singh, A. K., Petrology and geochemistry of Abyssal peridotites from the Manipur Ophiolite Complex, Indo-Myanmar Orogenic Belt, Northeast India: Implication for melt generation in mid-oceanic ridge environment. *J. Earth Sci*., 2013, **66**, 258–276.
8. Singh, I., Devi, L. D. and Chanu, Th. Y., Petrological and geochemical study of serpentinized peridotites from the southern part of Manipur Ophiolite Complex, Northeast India. *J. Geol. Soc. India*, 2013, **82**, 121–132.
9. Ghose, N. C., Chatterjee, N. and Fareeduddin, *A Petrographic Atlas of an Ophiolite: An Example from the Eastern India-Asia Collision Zone*, Springer, New Delhi, 2014, p. 234.
10. Ghosh, B., Ray, J. and Morishita, T., Grain-scale plastic deformation of chromite from podiform chromitite of the Naga–Manipur Ophiolite belt, India: implication to mantle dynamics. *Ore Geol. Rev.*, 2014, **56**, 199–208.
11. Pal, T., Bhattarcharya, A., Nagendran, G., Yanthan, N. M., Singh, R. and Raghumani, N., Petrogenesis of chromites from the Manipur belt, NE India: evidence for a supra-subduction zone setting prior to Indo-Myanmar collision. *Mineral. Petrol*., 2014, **108**, 713–726.
12. Khogenkumar, S., Singh, A. K., Singh, R. K. B., Khanna, P. P., Singh, N. I. and Singh, W. I., Coexistence of MORB and OIB-type mafic volcanics in the Manipur Ophiolite Complex, Indo-Myanmar Orogenic Belt, Northeast India: Implication for heterogeneous mantle source at the spreading zone. *J. Asian Earth Sci.*, 2016, **116**, 42–58.
13. Gansser, A., The significance of the Himalayan suture zone in the alpine Himalayan Region (eds Tater, J. M.), *Tectonophysics*, 1980, **62**, 37–52.
14. Mitchell, A. H. G., Phanerozoic plate boundaries in mainland SE Asia, the Himalayas and Tibet. *J. Geol. Soc. London*, 1981, **138**, 109–122.
15. Acharyya, S. K., Ray, K. K. and Roy, D. K., Tectono-stratigraphy and emplacement history of the ophiolite assemblage from the Naga Hills and Andaman Island arc India. *J. Geol. Soc. India*, 1989, **33**, 4–18.
16. Ghose, N. C., Agarwal, O. P. and Singh, R. N., Geochemistry of the ophiolite belt of Nagaland, N.E. India. In *Ophiolite and Indian Plate Margin* (eds Ghose, N. C. and Varadarajan, S.), Sumna Publ., Patna, 1986, pp. 241–293.
17. Acharyya, S. K., Ray, K. K. and Roy, D. K., Tectono-stratigraphy and emplacement history of the ophiolite assemblage from the Naga Hills and Andaman Island Arc, India. *J. Geol. Soc. India*, 1989, **33**(1), 4–18.
18. Agarwal, O. P. and Kacker, R. N., Nagaland ophiolite, India: a subduction zone ophiolite complex in Tethyan orogenic belt, In *Ophiolites* (eds Panayiotoau, A.), Proceedings of International Ophiolite Symposium, Cyprus, 1979, pp. 454–461.
19. Bhattacharjee, C. C., The ophiolite of northeast India – a subduction zone ophiolite complex of the Indo-Burman orogenic belt. *Tectonophysics*, 1991, **191**, 213–222.
20. Nandy, D. R., *Geodynamics of Northeastern India and the Adjoining Regions*, ACB Publications, Block-A Lake Town, Kolkata, India, 2001, p. 757.
21. Ghose, N. C., Agarwal, O. P. and Chatterjee, N., Geological and mineralogical study of eclogite and glucophane schists in the Naga Ophiolite, Northeast India. *Island Arc*, 2010, **10**, 336–356.
22. Puga, E., Nieto, J. M., Diaz de Federico, A., Bodinier, J. L. and Morten, L., Petrology and metamorphic evolution of ultramafic rocks and dolerite dykes of the Betic Ophiolitic Association (Mulhacen Complex, SE Spain): evidence of eo-Alpine subduction following an ocean-floor metasomatic process. *Lithos*, 1999, **49**, 23–56.
23. Peltonen, P., Kontinen, A. and Huhma, H., Petrogenesis of the mantle sequence of Jormua Ophiolite (Finland): Melt migration in the Upper Mantle during Paleoproterozoic continental break-up. *J. Petrol*., 1998, **39**(2), 297–329.
24. Morimoto, N. and Kitamura, M., Q–J diagram for classification of pyroxenes. *J. Japanese Assoc. Mineral., Petrol. Ecol. Geol*., 1983, **78**, 141.
25. Morimoto, N., Fabries, J., Ferguson, A. K., Ginzburg, I. V., Ross, M., Seifert, F. A. and Zussman, J., Nomenclature of pyroxenes. *Am. Mineral*., 1988, **73**, 1123–1133.

26. Beccaluva, L., Macciotta, G., Piccardo, G. B. and Zeda, O., Clinopyroxene composition of ophiolite basalts as petrogenetic indicator. *Chem. Geol*., 1989, **77**(3), 165–182.
27. D'Antonio, M. and Kristensen, M. B., Serpentine and brucite of ultramafic clasts from the South Chamorro Seamount (Ocean Drilling Program Leg 196, Site1200): inferences for the serpentinization of the Mariana forearc mantle. *Min. Mag.*, 2004, **68**, 887–904.
28. Lindsley, D. H., Pyroxene thermometry. *Am. Mineral*., 1983, **68**, 477–493.
29. Nimis, P., A clinopyroxene geobarometer for basaltic systems based on crystal–structure modeling. *Contrib. Mineral. Petrol*., 1995, **121**, 115–125.
30. Barnes, S. J. and Roeder, P. L., The range of spinel compositions in terrestrial mafic and ultramafic rocks. *J. Petrol*., 2001, **42**, 2279–2302.
31. Ohara, Y., Stern, R. J., Ishii, T., Yurimoto, H. and Yamazaki, T., Peridotites from the Mariana trough: first look at the mantle beneath an active back-arc basin. *Contrib. Mineral. Petrol*., 2002, **143**, 1–18.
32. Bonatti, E. and Michael, P. J., Mantle peridotites from continental rifts to ocean basins to subduction zones. *Earth Planet. Sci*., 1989, **91**, 297–311.
33. Arai, S., Characterization of spinel peridotites by olivine-spinel compositional relationships: review and interpretation. *Chem. Geol*., **113**, 191–204.
34. Varfalvy, V. and Hebert, R., Petrology and geochemistry of the pyroxenite dykes in the upper mantle peridotites of the Northern Arm Mountain Massif, Bay of Islands Ophiolite, Newfoundland: implication for the genesis of boninitic and related magmas. *Can. Mineral.*, 1997, **135**, 543–570.
35. Schwartz, S. *et al.*, Pressure-temperature estimates of the lizardite/antigorite transition in high pressure serpentinites. *Lithos*, 2013, **178**, 197–210.
36. Saccani, E. and Photiades, A., Mid-ocean ridge and supra-subduction affinities in the Pindos ophiolites (Greece): implication for magma genesis in a forearc setting. *Lithos*, 2004, **73**, 229–253.
37. Dick, H. J. B. and Bullen, T., Cr-spinel as a petrogenetic indicator in abyssal and alpine-type peridotites and spatially associated lavas. *Contrib. Mineral. Petrol*., 1984, **86**, 54–76.
38. Jan, M. Q. and Windley, B. F., Chromian spinel-silicate chemistry in ultramafic rocks of the Jijal complex, Northwest Pakistan. *J. Petrol*., 1990, **31**, 667–715.
39. Arai, S., Chemistry of chromian spinel in volcanic rocks as a potential guide to magma chemistry. *Mineral. Mag*., 1992, **56**, 173–184.
40. Ishii, T., Robinson, P. T., Maekawa, H. and Fisk, R., Petrological studies of peridotites from diapiric serpentinite seamounts in the Izu-Ogasawara-Mariana forearc, Leg 125, Proceedings of the Ocean Drilling Program, Scientific Results, 1992, **125**, 445–485.
41. Hirose, K. and Kawamoto, T., Hydrous partial melting of lherzolite at 1 Gpa: the effect of H_2O on the genesis of basaltic magmas. *Earth Planet. Sci. Lett*., 1995, **133**, 463–473.
42. Kamenetsky, V. S., Crawford, A. J. and Meffre, S., Factors controlling chemistry of magmatic spinel: an empirical study of associated olivine, Cr-spinel and melt inclusions from primitive rocks. *J. Petrol*., 2001, **42**, 655–671.

ACKNOWLEDGEMENTS. We thank DST, New Delhi for financial support (Grant No: SR/S4/ES-389/2008). We also thank the anonymous reviewers for their incisive comments that helped improve the manuscript.

Received 30 July 2016; revised accepted 29 November 2016

doi: 10.18520/cs/v112/i10/2122-2129

Interactions of lion-tailed macaque (*Macaca silenus*) with non-primates in the Western Ghats, India

Joseph J. Erinjery[1], Honnavalli N. Kumara[2], K. Mohan[1] and Mewa Singh[1,3,4,*]

[1]Bio-Psychology Laboratory and Institute of Excellence, University of Mysore, Mysuru 570 006, India
[2]Sálim Ali Centre for Ornithology and Natural History, Coimbatore 641 108, India
[3]Evolutionary and Organismal Biology Unit, Jawaharlal Nehru Centre for Advanced Scientific Research, Bengaluru 560 064, India
[4]National Institute of Advanced Studies, Indian Institute of Science Campus, Bengaluru 560 012, India

Primates and non-primates inhabiting tropical forests may interact with each other since they coexist in the same communities. Primates usually interact with their prey, predators, competitors and neutral species. Using 'all occurrence' sampling, we have studied inter-specific interactions of lion-tailed macaques with non-primate species found in their habitat. We observed that the percentage of total time spent on interactions with non-primates was less than 1. Also, the percentage of total time spent in interacting with competitors, predators and neutral species was less than 0.5. The lack of predation pressure and lack of opportunities for mixed-species associations for increasing foraging efficiency appear to be the major reasons for the absence of interactions with non-primates. By comparing with studies from other primate habitat regions, we observed that primates in South Asia interact much lesser with non-primates than those in South America and Africa. A previous study showed that the interactions of lion-tailed macaques even with other primate species in the Western Ghats are less than expected by chance.

Keywords: Inter-specific competition, mixed-species troops, *Macaca silenus*, primate–predator interaction.

PRIMATES in tropical forests may interact with other non-primate species which coexist with them[1–3]. These interactions could be either positive, negative or neutral[4,5], and may vary with space and time[5–7], largely depending on ecological and historical factors which shape them. The primates mainly interact with their prey, predators, feeding competitors and neutral species, and may display a variety of behaviours towards an interacting species[5]. Most direct interactions such as aggression and submission occur when two species encounter in close proximity[8]. Long-distance interactions such as alarm calls and spacing calls are important for communication about detection of predators and foraging[9].

*For correspondence. (e-mail: mewasinghltm@gmail.com)